ADVANCED MATERIALS
www.advmat.de

Check for updates

Designed Growth of Large-Size 2D Single Crystals

*Can Liu, Li Wang, Jiajie Qi, and Kaihui Liu**

In the "post-Moore's Law" era, new materials are highly expected to bring next revolutionary technologies in electronics and optoelectronics, wherein 2D materials are considered as very promising candidates beyond bulk materials due to their superiorities of atomic thickness, excellent properties, full components, and the compatibility with the processing technologies of traditional complementary metal-oxide semiconductors, enabling great potential in fabrication of logic, storage, optoelectronic, and photonic 2D devices with better performances than state-of-the-art ones. Toward the massive applications of highly integrated 2D devices, large-size 2D single crystals are a prerequisite for the ultimate quality of materials and extreme uniformity of properties. However, at present, it is still very challenging to grow all 2D single crystals into the wafer scale. Therefore, a systematic understanding for controlled growth of various 2D single crystals needs to be further established. Here, four key aspects are reviewed, i.e., nucleation control, growth promotion, surface engineering, and phase control, which are expected to be controllable at different periods during the growth. In addition, the perspectives on designed growth and potential applications are discussed for showing the bright future of these advanced material systems of 2D single crystals.

1. Introduction

In the history of human civilization, materials science has worked as one of the main driving forces to proceed the development of social productivities. Particularly in past decades, various silicon-based devices have witnessed the progress and prosperity in modern information industry, especially in electronics and optoelectronics. Now we are entering a "post-Moore" era, and new materials are highly desired to launch the next industrial revolution to further boost our slower-growing social productivities. Therefore, intensive researches on potential materials candidates, such as strong-correlated materials, topological materials, and low-dimensional materials, are rising in the limelight. Wherein, 2D materials family are deemed to be a very promising choice due to their inherent superiorities: 1) atomic thickness, which was proved that can overcome the short-channel effect, and lower the energy consumption of devices effectively;[1–4] 2) excellent properties, such as the highest carrier mobility,[5,6] or ultrafast charge transfer between 2D interfaces[7] for high clock speed of devices, etc.; 3) full components, including conductor (graphene),[8] semiconductor (transition metal dichalcogenides, bilayer graphene, black phosphorus, etc.),[9–12] insulator (hexagonal boron nitride, known as hBN),[13,14] and magnet (CrI_3, Fe_3GeTe_2, etc.),[15–19] enabling the fabrication of 2D logic, storage, photoelectric, and photonic devices; and 4) the compatible processing techniques, enabling the manufacture of high integrated devices with 2D materials, just like that of the traditional complementary metal-oxide-semiconductors devices.[20–22] However, to realize the great potentials of integrated 2D devices, it is of big prerequisite to have the materials of large-size 2D single crystals because only large-size single crystals could provide the ultimate quality of materials without evident worsening from the defective grain boundaries and also the extreme uniformity of properties on account of the strict lattice periodicity over a wide range, which is very necessary for large scale integration. Therefore, growth of large-size 2D single crystals is of great significance and urgency.

To grow the ideal 2D single crystals, it is natural to learn from former experiences on preparation of bulk 3D single crystals. Unfortunately, it has turned out that many of previous methods in growth of 3D materials cannot be simply adopted, as 2D materials are about the atomic thickness, of which the preparation must rely on the surface of substrates. In general, typical approaches for growing bulk single crystals come from the solidification of melted polycrystalline ingots, such as Bridgman–Stockbarger method[23,24] and Czochralski process,[25] but it is nearly impossible to set a threshold in temperature gradient that allows the solidification of just one atomic layer to grow 2D single crystals. Even the multilayers of 2D materials are also extremely difficult to be grown in this way, owing to the weak van der Waals interaction between layers. On the other hand, it is very challenging to obtain the 2D single crystals just by annealing 2D polycrystals at high temperature, since the energy barriers for rotating 2D domains on substrate are too hard to reach.[26] As an interface system, in principle, the effective controls for growing 2D single crystals should be based

Dr. C. Liu, Dr. L. Wang, J. J. Qi, Prof. K. H. Liu
State Key Lab for Mesoscopic Physics
Frontiers Science Center for Nano-Optoelectronics
School of Physics
Peking University
Beijing 100871, China
E-mail: khliu@pku.edu.cn
Dr. L. Wang
Beijing National Laboratory for Condensed Matter Physics
Institute of Physics
Chinese Academy of Sciences
Beijing 100190, China
The ORCID identification number(s) for the author(s) of this article can be found under https://doi.org/10.1002/adma.202000046.

DOI: 10.1002/adma.202000046

 © 2020 WILEY-VCH Verlag GmbH & Co. KGaA, Weinheim

on the interfacial engineering between target 2D materials and the surface of substrates. Previously, many efforts have been devoted by this means, to proceed the designed growth of 2D single crystals to the limit of large size.[27,28] However, till now, only graphene and hBN could be prepared into sub-meter-size single crystals.[29,30] In view of this, a systematic understanding grounded on existing typical works needs to be further established to set the stage for future development in this field. Thereby, we have proposed and reviewed four key aspects, i.e., nucleation control, growth promotion, surface engineering, and phase control (**Figure 1**), which are expected that can be well controlled at different periods during the growth of various 2D materials. Moreover, the perspectives on preparations and applications of 2D single crystals are discussed, for showing the potential opportunities in realizing the technological revolution by 2D material system.

2. Controls of 2D Single-Crystal Growth

2.1. Nucleation Control

The nucleus, as well known, is the seed of crystallization for any material. In terms of 2D materials, nucleation commonly happens at the positions of high surface energy on substrates.[31–34] The initial nuclei formed on active sites tend to be randomly distributed and orientated if there are no effective means of controls applied, leading to massive grain boundaries, known as a kind of line defects, during the coalescence between these domains. The line defects in 2D materials would greatly degrade the electrical, thermal, and mechanical performance, and the homogeneousness of as-prepared 2D materials, to further hamper the high-end and industrial-level applications of 2D materials.[35–37] In past decade, numerous efforts have been devoted to suppress the nucleation density for preparing high-quality 2D single crystal from one single nucleus. All methods of such kinds of controls could be basically classified into two categories typically in strategy respect: 1) reducing the active sites of nucleation on the substrate and 2) selectively feeding single nucleus to evolve into large scale.

Since the excess nuclei stem from the active sites on substrate, it is natural to remove them by adopting some proper pretreatments to the substrates. Earlier many researchers found that single domain of graphene could be grown around millimeter size simply by folding the copper (Cu) foil substrate into the shape of envelope,[38] or annealing at high temperature for very long time,[39] or electrochemically polishing the surface.[40] Such kinds of pretreatments aim at passivating (or reducing) some active sites on the surfaces of industrial Cu foils, and most of which are the defects or impurities generated during the production process of raw Cu foil. To thoroughly eliminate them for growing large-size single domain, liquid Cu was employed to be an atomically smooth and pure substrate, verified to be able to reduce the nucleation rate and accelerate the growth of graphene domains to the great extent.[41,42] As can be seen specifically in **Figure 2**a, supporting plate of tungsten (W) or molybdenum (Mo) was used to prevent the melted Cu (directly placed or electroplated in advance) from balling for the strong surface tension. The nucleation density of graphene on the liquid Cu was obviously less than that on solid Cu substrate, and the as-grown hexagonal domains with small rotation angles presented a "self-assembly like" behavior for minimizing the surface/edge energy of graphene domains on liquid Cu surface (Figure 2b). Besides, the diffusion of dissociative carbons was intensified prominently on liquid Cu surface, resulting in the fast growth rate of 10–50 μm min^{-1}, two orders of magnitude higher than that on the Cu solid surface at similar growth conditions. Soon afterward, the growth of graphene on liquid gallium, indium, nickel, tin, and their alloys was carried out to confirm that liquid metal substrates were indeed an effective and universal way to control the nucleation of 2D materials.[43–45] Other than the direct regulations on metal foils, some exotic molecules were also applied to further decrease the number of potential nucleation centers on the surface of substrates. The oxidation of substrates had been widely

Can Liu is currently a postdoctoral research fellow in the School of Physics, Peking University, Beijing, China. She received her B.S. degree from Northwestern Polytechnical University in 2014 and her Ph.D. degree from Peking University in 2019. Her research interests mainly focus on the interfacial modulation growth of single-crystal 2D materials.

Li Wang is currently a postdoctoral research fellow in the Institute of Physics, Chinese Academy of Sciences, China. He received his B.S. and Ph.D. degrees from Wuhan University in 2009 and 2016, respectively. His research interest is focused on the synthesis and related applications of single-crystal 2D materials.

Kaihui Liu is currently a professor and principle investigator in the State Key Lab for Mesoscopic Physics, School of Physics, Peking University, China. He received his Ph.D. from the Institute of Physics, Chinese Academy of Sciences in 2009 and afterward worked as a postdoctoral research fellow at UC Berkeley, USA, until 2014. His current research interests are the growth, characterization, and applications of meter-scale single crystals.

 © 2020 WILEY-VCH Verlag GmbH & Co. KGaA, Weinheim

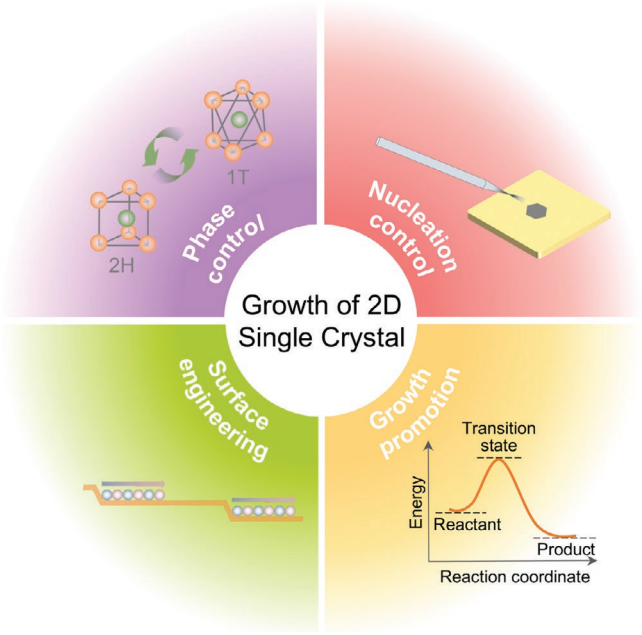

Figure 1. Schematic illustration of four key aspects for growth of 2D single crystals.

and thoroughly studied that can push the size of graphene domains forward to centimeter scale.[46–49] Moreover, it had been explored that decomposition of melamine to the carbon- and nitrogen-containing species could be catalyzed by the active sites on Cu surface, such as grain boundaries, to form a strong interaction between nitrogen/carbon and grain boundaries, and subsequently preclude the nucleation here due to an analogous effect of self-limited catalysis in graphene growth (Figure 2c).[50] It was observed that the nucleation density was lowered from 2 to 5×10^{-3} mm^{-2} (Figure 2d) with the melamine treatment, and thereby the centimeter-sized single-crystal graphene domains with carrier mobilities had exceeded 25 000 cm^2 V^{-1} s^{-1}, and even the Quantum Hall effect of graphene had been achieved. Amazingly, the carbon- and nitrogen-containing compounds were not residual on Cu foils with the full coverage of graphene film, and it could be confirmed through the X-ray photoelectron spectroscopy and the auger electron spectroscopy, disclosing the advantage that no contamination was brought by the exotic molecules. As for the growth of graphene on SiO_2, trace amount of water from the decomposition of precursor of methanol with the aid of O_2 released from SiO_2 could moderately hydroxylate the substrate to successfully suppress the secondary nucleation of graphene, resulting in the primary nucleation-dominated growth of large (360–860 nm) graphene domains on dielectric substrate.[51] Moreover, similar phenomena of the suppression of excess nucleation have been observed in the growth of MoS_2 by introducing the hydroxylation,[52] alkali metal halides,[53] oxygen,[54] or separating the induction stage from the growth stage.[55]

The ultimate goal for controlling the nucleation during the growth of 2D materials is to feed single nucleus to evolve into a single-crystal film of huge size. It is full of challenge as the process of nucleation is the "random event in the isolated system." To solve this problem, the approach of local precursor feeding was developed to make the nucleation just taken place at the fixed position, then super saturation of carbon source was continuously provided at the tiny area around it (Figure 2e). Through this design, monolayer graphene domain with the size of 1.5 in. was grown on Cu–Ni alloys in 2.5 h (Figure 2f).[56] The reason for choosing the substrate made of Cu–Ni alloy was changing the carbon diffusion mode from surface to quasi-3D for higher carbon solubility, as well as the growth mechanism from surface-mediated growth to isothermal segregation, and

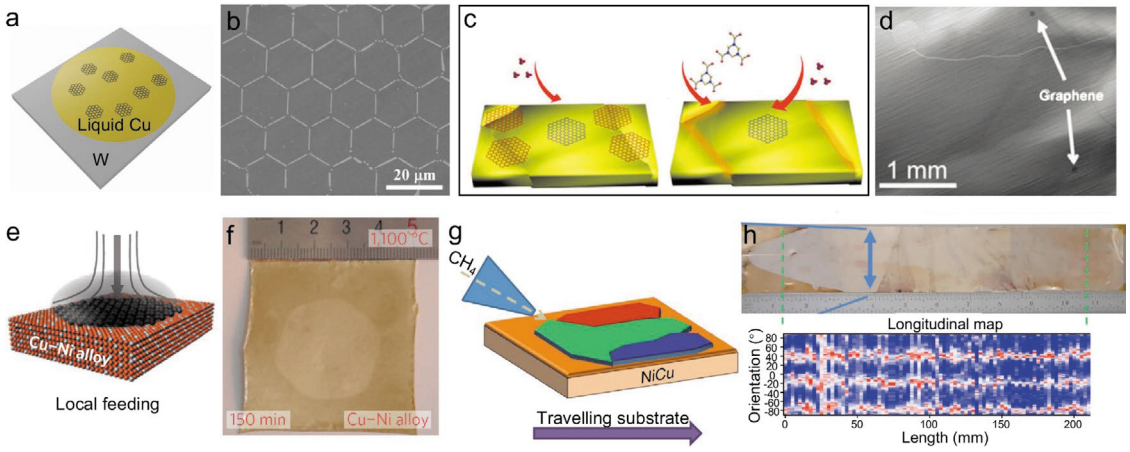

Figure 2. a–d) Nucleation control of 2D materials by pretreatment of the catalytic surface and e–h) growth from one individual nucleus. a) Schematic illustration of graphene grown on flat liquid Cu surface on W substrates. b) Scanning electron microscopic (SEM) image, showing the "self-assembly-like" behavior of hexagonal graphene domains on liquid Cu surface. a,b) Reproduced with permission.[41] Copyright 2012, National Academy of Sciences, USA. c) Schematic illustration of the passivation of the active sites on Cu by melamine to suppress the nucleation density. d) SEM image reveals the remarkable reduction of nucleation density of graphene domains. c,d) Reproduced with permission.[50] Copyright 2016, American Chemical Society. e) Schematic illustration of the design of the local-feeding method to control the formation of only one single nucleus on $Cu_{85}Ni_{15}$ substrate. f) Optical image of a ≈1.5 in. single-crystal graphene grown from one nucleus. e,f) Reproduced with permission.[56] Copyright 2015, Springer Nature. g) Schematic illustration of evolutionary selection growth of one faster domain. h) Photograph of a 1 foot long single crystal graphene with the direction of growth at about 20° with respect to the zigzag edge. g,h) Reproduced with permission.[57] Copyright 2018, Springer Nature.

© 2020 WILEY-VCH Verlag GmbH & Co. KGaA, Weinheim

increasing the growth rate. Based on this method, evolutionary selection of growth was realized by simultaneously pulling the substrate at desired speed during the growth by local precursor feeding and foot-long single-crystal-like monolayer graphene was synthesized on the polycrystalline substrate (Figure 2g,h).[57] High-velocity wind of the buffer gas and the Cu–Ni alloy substrate were two critical parameters to offer a sharp concentration gradient at the front and thus get rid of unwanted nucleation. This approach could be broadly utilized on other single-crystal 2D materials with different composition and symmetry in principle, and showing the very promising future in industrial production.

In all, effective controls on suppressing nucleation could be fulfilled simply by folding, long-time annealing or electrochemically polishing on the substrate of solid Cu foil. Besides, liquid metals and exotic molecules were also proved to be able to reduce the nucleation rate. By local-precursor-feeding approach, single nucleus of graphene could be grown into a single domain of 1.5 in. Foot-long single-crystal graphene film was realized via adding an evolutionary selection of growth, which was simultaneously pulling the substrate at desired speed during the growth by local precursor feeding.

2.2. Growth Promotion

During the process of single nucleus evolving into large single crystal, increase of growth rate is of equal importance as reduce of the nucleation rate, since faster growth of domains would further lower the appearance of new nuclei for shorter growth time and higher coverage. Besides, high growth rate could directly enhance the production of 2D single crystals, thus relevant studies with respect to growth dynamics to modulate the growth rate were considerably crucial and also provided the thorough understanding of growth mechanism. Typically, the evolvement of single nucleus contains two necessary steps during the growth, i.e., the decomposition and diffusion of feedstocks, the edge attachment of adatoms, which can usually be realized by 1) modulating the catalytic activity and 2) introducing active species.

As is well known, substrates of metals are commonly used as the catalyst during the reaction in chemical vapor deposition (CVD) growth of graphene or hBN. It had been found that the energy barriers of methane decomposition can be greatly lessened by replacing Cu atom with Ni atom on Cu(001) facet.[56] Recently, the catalytic behavior of Ni adatoms during the growth of graphene on Ni substrate was studied in situ in high-speed scanning tunneling microscopy (STM) combined with density functional theory (DFT) simulations.[58] **Figure 3**a,b displays two stable structures of the short-lived Ni adatom and one or two top C atoms at the kink sites, and the simulations results revealed that the rate-limiting energy barrier of the cyclic process had been reduced by ≈35%. Besides, to realize the fast-speed growth of transition metal dichalcogenides (TMDCs), metal-organic chemical vapor deposition (MOCVD) was proven to be an effective way. Through the designed precursors and processes of serial reactions during growth, energy barriers of serial reactions could be drastically reduced, so as to the growth rates were consequently boosted.[59–62]

The growth of 2D materials is the attachment of adatoms around the edges of 2D domains. It has been reported that the edge of graphene domain is zigzag because the addition of carbon atoms onto armchair edge of graphene is much faster than that onto zigzag edge during growth.[63,64] Theory calculations further revealed that hydrogen-terminated edges of graphene are more energetically favorable on Cu facets, thus the dehydrogenation of edge should be the initial step before the edge attachment of carbon. By introducing oxygen and forming OH group on the Cu surface, energy of H on Cu could be lowered by 0.6 eV per H (Figure 3c–e),[47] and by Bell–Evans–Polanyi principle the activation energy of edge dehydrogenation could be lowered accordingly. Moreover, oxygen was also proved that can catalyze the decomposition of hydrocarbon feedstock, then make for the acceleration of edge attachment of carbon. Continuous and proper dosing oxygen on catalyst surface was not easy due to the neutralization from hydrogen in CVD system. In response to this, a continuous oxygen supply with an adjacent quartz plate (≈15 μm away from Cu foil) was designed to continuously release oxygen by breaking the dangling bonds at the quartz surface (Figure 3f),[65] on which the released oxygen from quartz plate was confined in the narrow gap, resulting in the enhanced oxygen attachment to the surface of Cu. Single-crystal graphene domains of round shape with a lateral size of 0.3 mm were obtained in just 5 s with such oxygen assistance, several orders of magnitude faster than reported graphene growth rate without oxygen supply under the similar growth conditions at that moment. Analysis on the dissociating process of CH_4 on Cu(100) surface further revealed that the reaction barrier was greatly reduced by 0.95 eV (Figure 3g–i), on accounts of the drastically increased concentration of CH_3 radicles and the CH_2, CH, and C accordingly by the dissociation of serial hydrocarbons. Lately, such local-element-feeding method was developed by employing fluorine, a more active species but with different functions compared to that of oxygen on Cu surface. Fluorine released from metal fluoride surface could substitute the hydrogen in CH_4 easily in the gas phase (Figure 3j,k), leading to a locally high concentration of CH_3F in the similar narrow gap between fluoride and Cu surface. Furthermore, the decomposition of CH_3F on the Cu surface was highly energy favorable (switching the reaction type from endothermic to exothermic ones) and much easier than that of CH_4 on Cu surface owing to the decreased energy barrier (≈0.33 eV) (Figure 3l). For these reasons, growth rate of graphene had reached the highest level of ≈200 μm s^{-1} with the assistance of fluorine.[66] This method of accelerating growth of graphene via local element supply can be also applied to other 2D materials such as hBN and WS_2, which turned out to be a universal kinetic and thermodynamic modulation method for surface growth and interfacial engineering.

In short, studies on growth dynamics of 2D materials aimed at the promotion of growth rate, to prepare much larger 2D single crystal from single nucleus. The Ni atoms were found that can increase the growth rate of graphene and hBN by lowering the energy barrier of the reaction during growth. Besides, to fast grow large-scale TMDCs, MOCVD was proven to be a very promising method. In addition, the assistance of oxygen and fluorine supplied in confined narrow gap could boost the

© 2020 WILEY-VCH Verlag GmbH & Co. KGaA, Weinheim

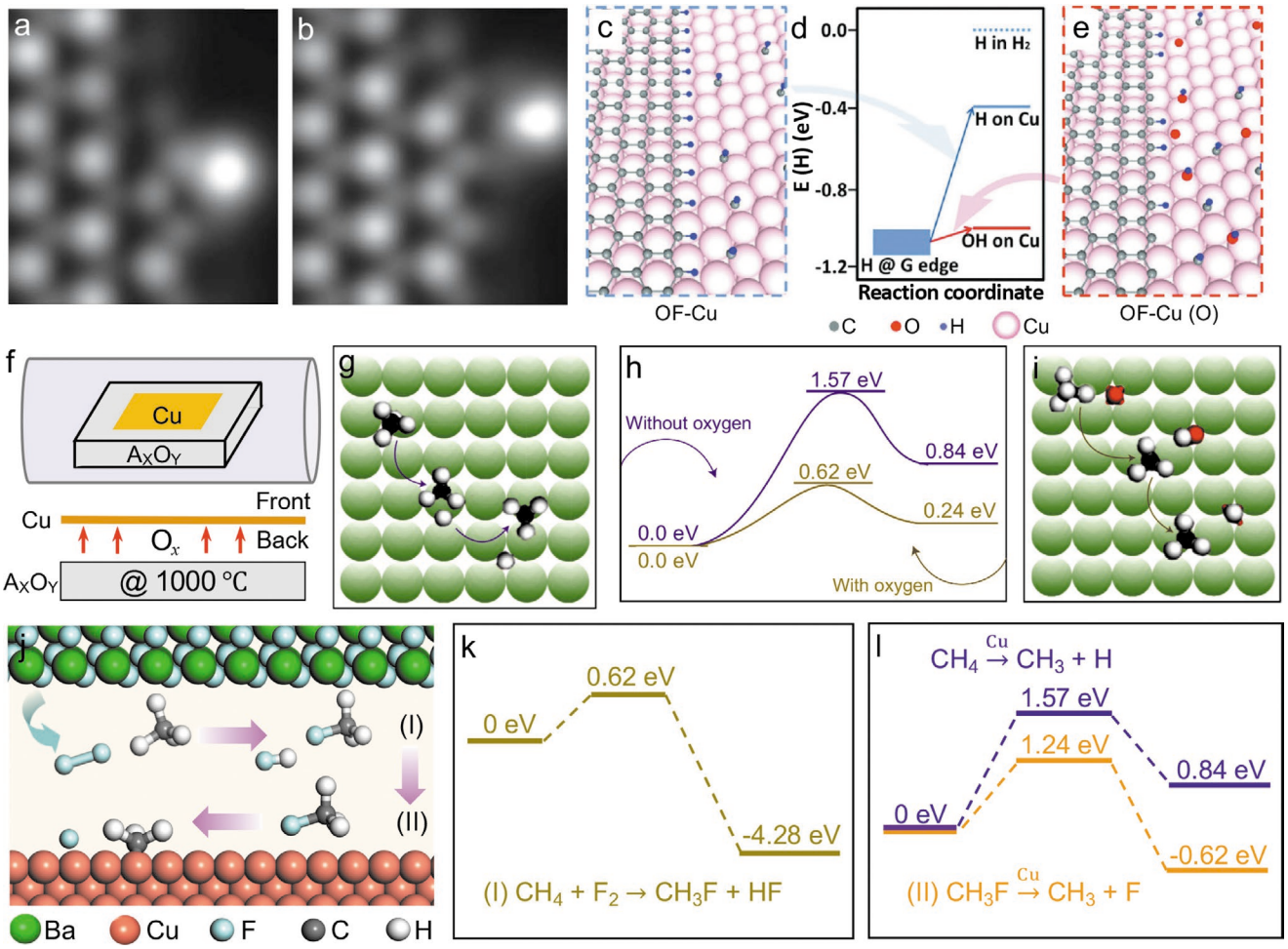

Figure 3. Growth promotion of 2D materials through the modulation of growth dynamics. a,b) STM simulated images of the Ni adatoms at the graphene edges. a,b) Reproduced with permission.[58] Copyright 2018, American Association for the Advancement of Science (AAAS). c–e) Atomic-scale schematics of graphene edges grown on Cu with (e) and without (c) oxygen and d) the corresponding DFT calculations of the energies for H attachment. c–e) Reproduced with permission.[47] Copyright 2013, AAAS. f) Schematic illustration of the experimental design of local-oxygen-feeding method. g–i) The energy profiles of CH_4 decomposition reaction i) with and g) without oxygen supply on Cu surface. f–i) Reproduced with permission.[65] Copyright 2016, Springer Nature. j) One possible decomposition route and k,l) the corresponding energy profile of carbon species with the assistance of local fluorine. j–l) Reproduced with permission.[66] Copyright 2019, Springer Nature.

growth rate tremendously by promoting the edge dehydrogenation and decomposition of the hydrocarbons as well.

2.3. Surface Engineering

Single nucleus of graphene was proven that can evolve into a large-size graphene film, with the separate gas stream by nozzle for dosing.[56,57] However, similar approach has not been successfully duplicated on other 2D materials yet, mainly because of the extreme difficulty in generally suppressing the nucleation rate to the very low level. In this case, domains certainly would coalesce before their sizes could be enlarged satisfactorily, therefore 2D single crystals are expected to be prepared through the seamless stitching of multiple domains by epitaxial method. Earlier in the case of graphene grown on Ge(110) and Cu(111), experimental evidences have been given that two graphene domains with same orientation could be stitched seamlessly without grain boundary.[67,68] It has been reported that the orientations of domains could be determined by the surface symmetry of substrate, since the energetically preferential orientations of nuclei would be reproduced by the symmetric operation of the substrate through their interlayer van der Waals interaction. Thereby, the "surface engineering" focus on matching the lattice symmetry between substrate and 2D materials, by choosing or making the substrate with 1) same symmetry, 2) no symmetry, or 3) broken symmetry.

It is obvious that the simplest "surface engineering" is to choose a substrate with same surface symmetry to that of 2D materials. Accordingly, the epitaxial growth of half-meter-size single-crystal graphene was realized on single-crystal Cu(111) foil via seamless stitching of tens of thousands of the unidirectionally aligned graphene domains (**Figure 4**a).[30] In addition, the low-energy electron diffraction (LEED) patterns of graphene and Cu(111) (Figure 4b,c) demonstrated that they are of the same lattice orientation. Besides, unidirectionally aligned MoS_2

© 2020 WILEY-VCH Verlag GmbH & Co. KGaA, Weinheim

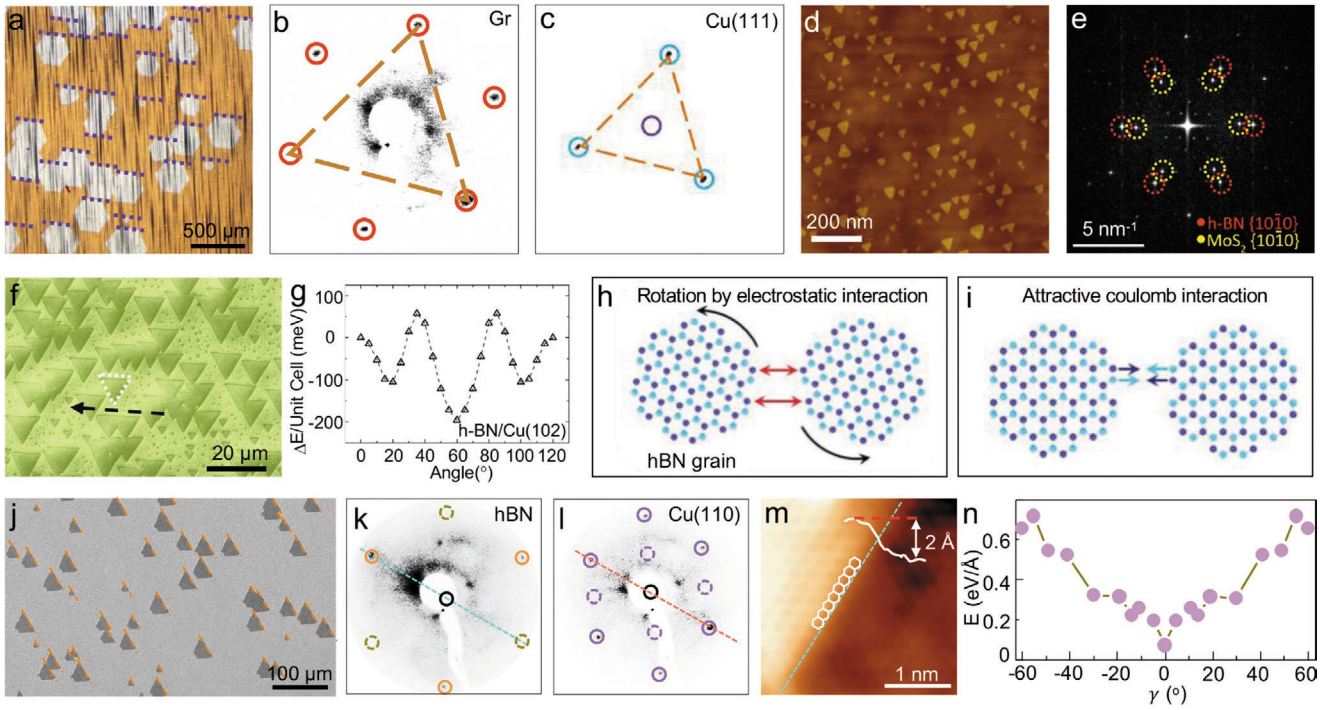

Figure 4. Growth of unidirectionally aligned 2D domains through surface engineering of substrate. a) Optical image of unidirectionally aligned graphene domains grown on Cu(111). b,c) LEED patterns of as-grown graphene (b) and Cu(111) (c). a–c) Reproduced with permission.[30] Copyright 2017, Elsevier. d) Atomic force microscopy (AFM) image of aligned MoS_2 domains grown on hBN flake. e) The fast Fourier transform (FFT) patterns of MoS_2/hBN heterostructure taken by scanning transmission electron microscopy (STEM), showing the identical lattice orientation of MoS_2 and hBN. d,e) Reproduced with permission.[69] Copyright 2017, American Chemical Society. f) SEM image of unidirectionally aligned hBN domains grown on Cu(102) with the electron backscattered diffraction background (EBSD) color of Cu(102). g) Calculated energies of hBN rotating on Cu(102), in which angle of 60° is the most energetically favorable. f,g) Reproduced with permission.[71] Copyright 2016, Wiley-VCH. h,i) Schematic illustration of the self-collimated rotation of round hBN domains. h,i) Reproduced with permission.[74] Copyright 2018, AAAS. j) SEM image of unidirectionally aligned hBN domains grown on Cu(110). k,l) LEED patterns of as-grown hBN (k) and Cu(110) (l). m) Atomically resolved STM image of a hBN covered Cu(110) terrace, showing the zigzag edge of hBN aligned to the atomic step on Cu surface. n) First-principles DFT calculations of the formation energies of hBN edges attached to the Cu<211> step edge on Cu(110) with respect to different rotation angle, showing that N-zigzag edge of hBN domain attaching to Cu<211> step edge is the most energetically favorable. j–n) Reproduced with permission.[29] Copyright 2019, Springer Nature.

domains with the alignment greater than 90% were grown on an hBN flake (Figure 4d) by the same means,[69] and no rotation angle between aligned MoS_2 domains and hBN flake could be observed in the selected area electron diffraction (SAED) patterns (Figure 4e). However, the commonly used Cu(111), with a centrosymmetric lattice on its top layer, has been proved to be the inappropriate substrate to grow the single-crystal hBN of non-centrosymmetric lattice, for bringing on the numerous antiparallel domains and twin grain boundaries during the coalescence of domains.[70] In view of this, some high-index Cu facets, such as Cu(102) and Cu(103), were selected to provide onefold symmetry (C_1) to eliminate the excess preferential orientations of hBN domains reproduced by multifold symmetry of substrate (Figure 4f).[71] Theoretical calculation had confirmed that the single orientation of hBN domains on Cu(102) and Cu(103) came from the exclusively energetic minimum (Figure 4g). Unfortunately it is unpractical for using Cu(102) and Cu(103) to produce large-size single-crystal hBN, because large-size single-crystal Cu foil with such scarce high-index facets is very hard to be prepared for their high formation energy.

As the surface symmetry of substrate is from periodicity of their lattice, the restrictions from symmetry of substrate could be broken by employing the noncrystalline substrates such as the liquid metals. So far, various growth mechanisms for self-aligned graphene grown on liquid Cu were studied.[41,72,73] In comparison, growth of self-aligned hBN domains is more difficult but also realized not long ago.[74] The substrate of liquid gold was chosen for the low solubility of B and N, and high diffusion of adatoms on the surface. Through optimizing the growth parameters, plenty of hBN domains with the round shape and similar size around 14.5 μm were closely packed. Afterward, the electrostatic interaction between N and B atoms at the edge of difference grains made all of them rotated into the same orientation (Figure 4h,i), then seamlessly stitched into a 3 cm size single-crystal hBN film eventually.

Despite the liquid gold, still the solid metals were widely believed to be the very important substrates for controlling the orientation of 2D domains directly and stably. It is worth mentioning that large-size single-crystal hBN was of the most significance and urgency for the time, since the other 2D single crystals with non-centrosymmetric lattice, such as TMDCs, could be epitaxially grown on it.[74] Through the well-designed annealing approach, a 10 cm × 10 cm single-crystal Cu(110) foil with vicinal surface was reported to be prepared from commercial polycrystalline Cu foils, then unidirectionally aligned hBN

© 2020 WILEY-VCH Verlag GmbH & Co. KGaA, Weinheim

domains with truncated triangle shape were grown within the area of 100 cm^2 for the first time (Figure 4j).[29] Moreover, LEED patterns (Figure 4k,l) of hBN and Cu(110) exhibited the single-crystal nature and distinct lattice symmetry between them. In combination with STM scanning (Figure 4m), it could be determined that the zigzag direction in hBN lattice was parallel to the atomic step edge (if the steps were too high, overlapping grain boundaries would be generated) along <211> direction on Cu(110). First principle calculations (Figure 4n) had confirmed that the interaction between N-terminate zigzag edge of hBN and atomic step edge along Cu<211> direction broke the energetic symmetry of antiparallel hBN domains grown on Cu(110), leading to the unidirectionally aligned growth of hBN domains, and seamlessly stitching into the large-size single-crystal monolayer finally. Such method of breaking the surface symmetry of substrates by artificially constructed steps exhibited the great potential to be broadly applied to the epitaxial growth of other large-area 2D single crystals as well.[75]

In brief, 2D domains with same orientation could seamlessly stitch into an entire piece of 2D single crystal. On this basis, for solid substrate, numerous unidirectionally aligned 2D domains could be obtained when the symmetry group of the surface of substrate is the subgroup of that of target 2D materials; for the liquid substrate, growth of unidirectionally aligned 2D domains could be also realized through some special mechanism, such as the self-collimated grain formation.

2.4. Phase Control

The well controls of nucleation density, growth rate, and the surface symmetry of substrates could ensure the preparation of single-crystal graphene or hBN as mentioned above; however, for the 2D materials that single layer consists of the vertically stacked multilayers of atoms, such as the TMDCs, phase control is also a nonnegligible aspect for the single-crystal preparation. To be specific, transition metal atoms in TMDCs are sandwiched between two layers of chalcogen atoms in coordination of either trigonal prismatic structure (known as the 2H phase) or octahedral structure (known as the 1T phase), and the 1T phase has some derivatives such as 1T' and 1T," for the different bonding formations of transition metals, depending on the lattice stability. Usually, TMDCs of 2H phase are of semiconductors, while the TMDCs of 1T (1T', 1T," etc.) are metallic. This unique feature could provide an alterable metal–semiconductor junction with an ultralow contact barrier[76] by the same compound but just distinct phases. Broad applications based on the novel feature of TMDCs must rely on the accurate phase controls toward single crystals, which could be classified into two ways in general: 1) phase transition and 2) direct growth.

Usually, there is always one phase of the more stable structure (usually it is 2H) that can be directly grown with the regular approaches, while synthesis of another metastable phase (usually it is 1T or 1T') counted on the transition from the as-grown stable phase. Technically, phases of TMDCs could be characterized by many methods such as electrical transport, photoluminescence, Raman or second harmonic generation for the different properties.[77,78] At the atomic scale, scanning transmission electron microscopy (STEM) could not only display the atomic structure of each phase directly but also be applied to controllably grow MoS_2 domain of 1T phase inside the 2H phase layer with the assistance of electron beam.[79] It was proposed that beam-induced phase transition is from the in-plane charge redistribution due to the electron excitation with vacancies formation, and associated mechanical strain.[80] In particular, strain was proved to have the influence on transition temperature (T_P), with tensile strain of 2%, the T_P of $MoTe_2$ could be tuned down to room temperature.[81] In theory, the energy barriers (ΔE) in phase transition of TMDCs from 2H to 1T were evaluated to be $\Delta E[MoS_2] > \Delta E[MoSe_2] > \Delta E[MoTe_2]$.[82,83] By charge injection, 1T phase would be stabilized considerably, and thereby ΔE could be drastically reduced to the level that can be easily overcome.[84] It was found that weak Ar-plasma treatment is also able to induce the phase transition of MoS_2 (**Figure 5**a,b).[85] Besides, intercalation of alkali metals (potassium, sodium, and lithium) ions were also proved to be an effective way and frequently used in the phase engineering of TMDCs in many previous works.[76,86,87]

Although post process of as-prepared 2H phase can take the TMDCs to the 1T (or 1T') phase, direct-growth approaches, especially in CVD system, still get the upper hand for the single-crystal preparation with ultrahigh phase purity and quality. Taking $MoTe_2$ as an example, it has been reported that good phase selectivity (or phase purity) could be realized by choosing the appropriate growth parameters, such as the growth and quench temperatures,[88] precursors and promoter,[89] or carrier gas flow rate and reaction temperature.[90] It is worth noting that by DFT calculations, the 1T' phase of $MoTe_2$ is more stable when Te vacancy is greater than 2%, therefore 1T' phase was commonly observed to be first appeared during the CVD growth. By extending the growth time, round domains of 2H phase started to emerge and can be evolved to few millimeters scale, or coalesced into a uniform $MoTe_2$ film with centimeter size (Figure 5c).[91] On the other side, direct CVD growth of MoS_2 with 1T phase is relatively harder than that of $MoTe_2$ owing to much higher nucleation energy of the unstable 1T phase.[92] Separate nanosized domains of 2H and 1T' phase MoS_2 were grown on Au(111) in molecular beam epitaxy system, and a topological insulator type behavior of 1T' phase MoS_2 was revealed.[93] By a well-designed approach of two-steps reactions between K_2MoO_4 and S powder, MoS_2 of 1T' phase could be synthesized with the size of hundreds of micrometers (Figure 5d–f), and transition to 2H phase in patterned area was induced by laser.[94] Here, the calculation results showed that the stability of 1T (1T') MoS_2 was deeply enhanced by introducing the potassium (K), so the phase-selective growth of MoS_2 could be realized on the adequate evaluation of the efficacy of the alkali metals ions. Further calculation indicated that 1T' phase of MoS_2 is more stable when K concentration exceeds 44% (Figure 5g).[95] In practice, the production of K, could be precisely controlled by tuning the ratio of H_2 (reductive) and Ar (inert) in atmosphere, to further regulate two different decomposition reactions of K_2MoS_4. Thus, the phase of as-grown MoS_2 could be controlled simply by adjusting the temperature and H_2 concentration during the growth (Figure 5h).

In total, phase control is very significant for single-crystal growth of TMDCs. Electron beam, strain, plasma treatment, charge injection, and intercalation by alkali metals ions are the

© 2020 WILEY-VCH Verlag GmbH & Co. KGaA, Weinheim

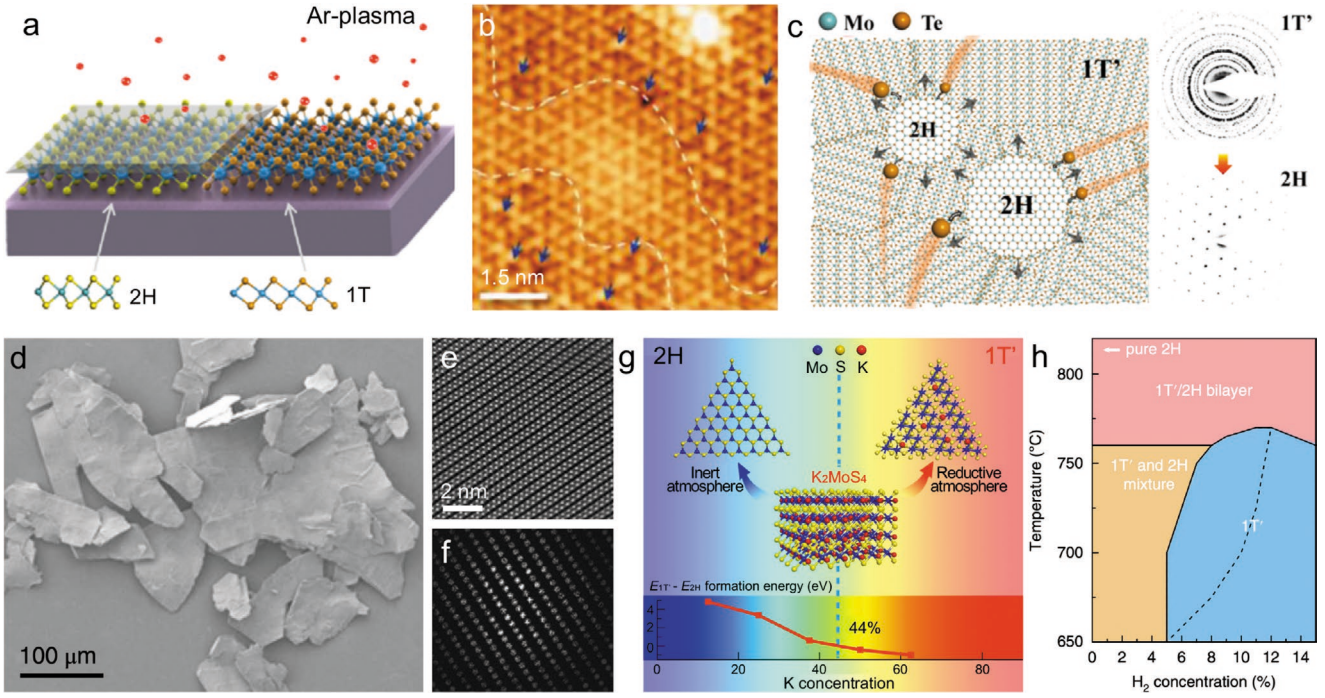

Figure 5. a,b) Phase control of TMDCs through phase transition and c–h) direct growth of the single-phase TMDCs. a) Schematic illustration of the phase transition of MoS_2 from 2H to 1T via Ar-plasma treatment. b) Atomically resolved STM image showing the phase transition of MoS_2, in which the boundaries between two phases are displayed by white dashed lines. a,b) Reproduced with permission.[85] Copyright 2017, American Chemical Society. c) Schematic illustration of phase selection during the growth of 2H-$MoTe_2$ through the recrystallization at the boundaries, and a set of SAED pattern of single-crystal 2H-$MoTe_2$ and a series of diffraction rings of 1T'-$MoTe_2$ shown at right side. c) Reproduced with permission.[91] Copyright 2019, American Chemical Society. d) SEM image of as-synthesized MoS_2 of 1T' phase. e) Atomically resolved STEM image of as-synthesized MoS_2 of 1T' phase and f) the corresponding FFT pattern. d–f) Reproduced with permission.[94] Copyright 2018, Springer Nature. g) Strategy of phase-selective growth of MoS_2 and formation-energy difference of K_xMoS_2 with respect to potassium concentration exhibited at the bottom. h) Phase diagram of MoS_2 grown from K_2MoS_2 with respect to H_2 concentration and growth temperature. g,h) Reproduced with permission.[95] Copyright 2018, Springer Nature.

commonly used ways for inducing phase transition. And by introducing the deficiency of Te and tuning the concentration of potassium in reactions, phase-selective growth of $MoTe_2$ and MoS_2 could be realized directly in CVD system, respectively.

3. Conclusion and Prospective

To sum up, four key aspects corresponding to the different stages for controlled growth of 2D single crystals have been introduced and discussed. The nucleation control, combined with growth promotion would lead to the growth of large-size 2D single crystal from single nucleus; the surface engineering could make all domains orientated unidirectionally, then stitched seamlessly into a large-size single-crystal film on the substrate with proper surface symmetry; phase control aims at the phase purity, namely the homogeneousness of lattice and properties of as-grown 2D single crystals. At this point, previous understanding toward the growth of large-size 2D single crystal has been moving toward systematization.

Among all 2D materials, just graphene and hBN have been reported for the single-crystal size exceeding sub-meter scale through the controlled growth on large-size single-crystal Cu foil with proper surface symmetry.[29,30] In view of this, to realize the mass production of more lager-size 2D single crystals, designing their exclusive substrate then annealing it into a larger-size single crystal, in association with suppressing the nucleation rate and promoting the growth rate seems to be a sound and all-round way. In addition, the as-grown 2D single crystals could be used as the substrate to grow single-crystal adlayers through their interlayer coupling, to build the multilayer 2D single crystals or vertical heterostructures with customized lattice configurations, such as the bilayer graphene of magic angle.[96,97] Moreover, some functional nanomaterials with controllable number of layers and morphology could be prepared from the templates of monolayer 2D single crystal as well. Besides, 2D single crystals hold the immense potential that can fabricate the full 2D devices in electronics and optoelectronics. These devices could perform high clock speed on account of the highest carrier mobility and ultrafast interlayer charge transfer, or wearable due to the inherent flexibility of 2D materials, or highly integrated for the compatible manufacturing process, etc. So, we believe that the very bright future of the technological revolution based on 2D single crystals will come sooner or later.

Acknowledgements

C.L., L.W., and J.J.Q. contributed equally to this work. This work was supported by Beijing Natural Science Foundation (JQ19004), Beijing excellent talents training support—top young individual project (2017000026833ZK11), the National Key R&D Program of China

© 2020 WILEY-VCH Verlag GmbH & Co. KGaA, Weinheim

(2016YFA0300903 and 2016YFA0300804), the National Natural Science Foundation of China (51991340 and 51991342), the Key R&D Program of Guangdong Province (2019B010931001 and 2018B030327001), Beijing Municipal Science and Technology Commission (Z191100007219005), Beijing Graphene Innovation Program (Z181100004818003), National Equipment Program of China (ZDYZ2015-1), Bureau of Industry and Information Technology of Shenzhen (No. 201901161512), National Postdoctoral Program for Innovative Talents (BX20190016), and China Postdoctoral Science Foundation (2019M660280).

Conflict of Interest

The authors declare no conflict of interest.

Keywords

2D materials, growth promotion, nucleation control, phase control, single crystals, surface engineering

Received: January 3, 2020
Revised: February 20, 2020
Published online:

[1] A. K. Geim, K. S. Novoselov, *Nat. Mater.* **2007**, *6*, 183.
[2] K. S. Novoselov, V. I. Fal'ko, L. Colombo, P. R. Gellert, M. G. Schwab, K. Kim, *Nature* **2012**, *490*, 192.
[3] S. B. Desai, S. R. Madhvapathy, A. B. Sachid, J. P. Llinas, Q. X. Wang, G. H. Ahn, G. Pitner, M. J. Kim, J. Bokor, C. M. Hu, H. S. P. Wong, A. Javey, *Science* **2016**, *354*, 99.
[4] M. Y. Li, S. K. Su, H. S. P. Wong, L. J. Li, *Nature* **2019**, *567*, 169.
[5] L. Banszerus, M. Schmitz, S. Engels, J. Dauber, M. Oellers, F. Haupt, K. Watanabe, T. Taniguchi, B. Beschoten, C. Stampfer, *Sci. Adv.* **2015**, *1*, e1500222.
[6] K. Kang, S. E. Xie, L. J. Huang, Y. M. Han, P. Y. Huang, K. F. Mak, C. J. Kim, D. Muller, J. Park, *Nature* **2015**, *520*, 656.
[7] K. S. Novoselov, A. Mishchenko, A. Carvalho, A. H. Castro Neto, *Science* **2016**, *353*, aac9439.
[8] K. S. Novoselov, A. K. Geim, S. V. Morozov, D. Jiang, Y. Zhang, S. V. Dubonos, I. V. Grigorieva, A. A. Firsov, *Science* **2004**, *306*, 666.
[9] F. Wang, Y. Zhang, C. Tian, C. Girit, A. Zettl, M. Crommie, Y. R. Shen, *Science* **2008**, *320*, 206.
[10] A. Carvalho, M. Wang, X. Zhu, A. S. Rodin, H. Su, A. H. Castro Neto, *Nat. Rev. Mater.* **2016**, *1*, 16061.
[11] S. Manzeli, D. Ovchinnikov, D. Pasquier, O. V. Yazyev, A. Kis, *Nat. Rev. Mater.* **2017**, *2*, 17033.
[12] B. L. Liu, Y. Q. Ma, A. Y. Zhang, L. Chen, A. N. Abbas, Y. H. Liu, C. F. Shen, H. C. Wan, C. W. Zhou, *ACS Nano* **2016**, *10*, 5153.
[13] K. Watanabe, T. Taniguchi, H. Kanda, *Nat. Mater.* **2004**, *3*, 404.
[14] M. S. Xu, T. Liang, M. M. Shi, H. Z. Chen, *Chem. Rev.* **2013**, *113*, 3766.
[15] C. Gong, L. Li, Z. Li, H. Ji, A. Stern, Y. Xia, T. Cao, W. Bao, C. Wang, Y. Wang, Z. Q. Qiu, R. J. Cava, S. G. Louie, J. Xia, X. Zhang, *Nature* **2017**, *546*, 265.
[16] Y. Deng, Y. Yu, Y. Song, J. Zhang, N. Z. Wang, Z. Sun, Y. Yi, Y. Z. Wu, S. Wu, J. Zhu, J. Wang, X. H. Chen, Y. Zhang, *Nature* **2018**, *563*, 94.
[17] S. Jiang, L. Li, Z. Wang, K. F. Mak, J. Shan, *Nat. Nanotechnol.* **2018**, *13*, 549.
[18] B. Huang, G. Clark, D. R. Klein, D. MacNeill, E. Navarro-Moratalla, K. L. Seyler, N. Wilson, M. A. McGuire, D. H. Cobden, D. Xiao, W. Yao, P. Jarillo-Herrero, X. Xu, *Nat. Nanotechnol.* **2018**, *13*, 544.
[19] M. Gibertini, M. Koperski, A. F. Morpurgo, K. S. Novoselov, *Nat. Nanotechnol.* **2019**, *14*, 408.
[20] H. Yang, J. Heo, S. Park, H. J. Song, D. H. Seo, K. E. Byun, P. Kim, I. Yoo, H. J. Chung, K. Kim, *Science* **2012**, *336*, 1140.
[21] S. Goossens, G. Navickaite, C. Monasterio, S. Gupta, J. J. Piqueras, R. Pérez, G. Burwell, I. Nikitskiy, T. Lasanta, T. Galán, E. Puma, A. Centeno, A. Pesquera, A. Zurutuza, G. Konstantatos, F. Koppens, *Nat. Photonics* **2017**, *11*, 366.
[22] L. F. Sun, Y. S. Zhang, G. Han, G. Hwang, J. B. Jiang, B. Joo, K. Watanabe, T. Taniguchi, Y. M. Kim, W. J. Yu, B. S. Kong, R. Zhao, H. Yang, *Nat. Commun.* **2019**, *10*, 3161.
[23] P. W. Bridgman, *Proc. Am. Acad. Arts Sci.* **1925**, *60*, 305.
[24] D. C. Stockbarger, *Rev. Sci. Instrum.* **1936**, *7*, 133.
[25] J. Czochralski, *Z. Phys. Chem.* **1917**, *92*, 219.
[26] R. Q. Zhao, X. L. Zhao, Z. R. Liu, F. Ding, Z. F. Liu, *Nanoscale* **2017**, *9*, 3561.
[27] Z. Y. Cai, B. L. Liu, X. L. Zou, H. M. Cheng, *Chem. Rev.* **2018**, *118*, 6091.
[28] J. Dong, L. Zhang, F. Ding, *Adv. Mater.* **2019**, *31*, 1801583.
[29] L. Wang, X. Z. Xu, L. N. Zhang, R. X. Qiao, M. H. Wu, Z. C. Wang, S. Zhang, J. Liang, Z. H. Zhang, Z. B. Zhang, W. Chen, X. D. Xie, J. Y. Zong, Y. W. Shan, Y. Guo, M. Willinger, H. Wu, Q. Y. Li, W. L. Wang, P. Gao, S. W. Wu, Y. Zhang, Y. Jiang, D. P. Yu, E. G. Wang, X. D. Bai, Z. J. Wang, F. Ding, K. H. Liu, *Nature* **2019**, *570*, 91.
[30] X. Z. Xu, Z. H. Zhang, J. C. Dong, D. Yi, J. J. Niu, M. H. Wu, L. Lin, R. K. Yin, M. Q. Li, J. Y. Zhou, S. X. Wang, J. L. Sun, X. J. Duan, P. Gao, Y. Jiang, X. S. Wu, H. L. Peng, R. S. Ruoff, Z. F. Liu, D. P. Yu, E. G. Wang, F. Ding, K. H. Liu, *Sci. Bull.* **2017**, *62*, 1074.
[31] B. Hammer, J. K. Norskov, *Nature* **1995**, *376*, 238.
[32] H. Chen, W. G. Zhu, Z. Y. Zhang, *Phys. Rev. Lett.* **2010**, *104*, 186101.
[33] J. F. Gao, J. Yip, J. J. Zhao, B. I. Yakobson, F. Ding, *J. Am. Chem. Soc.* **2011**, *133*, 5009.
[34] G. H. Han, F. Gunes, J. J. Bae, E. S. Kim, S. J. Chae, H. J. Shin, J. Y. Choi, D. Pribat, Y. H. Lee, *Nano Lett.* **2011**, *11*, 4144.
[35] Q. K. Yu, L. A. Jauregui, W. Wu, R. Colby, J. F. Tian, Z. H. Su, H. L. Cao, Z. H. Liu, D. Pandey, D. G. Wei, T. F. Chung, P. Peng, N. P. Guisinger, E. A. Stach, J. M. Bao, S. S. Pei, Y. P. Chen, *Nat. Mater.* **2011**, *10*, 443.
[36] P. Y. Huang, C. S. Ruiz-Vargas, A. M. van der Zande, W. S. Whitney, M. P. Levendorf, J. W. Kevek, S. Garg, J. S. Alden, C. J. Hustedt, Y. Zhu, J. Park, P. L. McEuen, D. A. Muller, *Nature* **2011**, *469*, 389.
[37] C. S. Ruiz-Vargas, H. L. L. Zhuang, P. Y. Huang, A. M. van der Zande, S. Garg, P. L. McEuen, D. A. Muller, R. G. Hennig, J. Park, *Nano Lett.* **2011**, *11*, 2259.
[38] X. S. Li, C. W. Magnuson, A. Venugopal, R. M. Tromp, J. B. Hannon, E. M. Vogel, L. Colombo, R. S. Ruoff, *J. Am. Chem. Soc.* **2011**, *133*, 2816.
[39] H. Wang, G. Z. Wang, P. F. Bao, S. L. Yang, W. Zhu, X. Xie, W. J. Zhang, *J. Am. Chem. Soc.* **2012**, *134*, 3627.
[40] Z. Yan, J. Lin, Z. W. Peng, Z. Z. Sun, Y. Zhu, L. Li, C. S. Xiang, E. L. Samuel, C. Kittrell, J. M. Tour, *ACS Nano* **2013**, *7*, 2872.
[41] D. C. Geng, B. Wu, Y. L. Guo, L. P. Huang, Y. Z. Xue, J. Y. Chen, G. Yu, L. Jiang, W. P. Hu, Y. Q. Liu, *Proc. Natl. Acad. Sci. USA* **2012**, *109*, 7992.
[42] Y. M. A. Wu, Y. Fan, S. Speller, G. L. Creeth, J. T. Sadowski, K. He, A. W. Robertson, C. S. Allen, J. H. Warner, *ACS Nano* **2012**, *6*, 5010.
[43] G. Q. Ding, Y. Zhu, S. M. Wang, Q. Gong, L. Sun, T. R. Wu, X. M. Xie, M. H. Jiang, *Carbon* **2013**, *53*, 321.
[44] M. Q. Zeng, L. F. Tan, J. Wang, L. F. Chen, M. H. Rummeli, L. Fu, *Chem. Mater.* **2014**, *26*, 3637.
[45] X. N. Zang, Q. Zhou, J. Y. Chang, K. S. Teh, M. S. Wei, A. Zettl, L. W. Lin, *Adv. Mater. Interfaces* **2017**, *4*, 1600783.
[46] H. L. Zhou, W. J. Yu, L. X. Liu, R. Cheng, Y. Chen, X. Q. Huang, Y. Liu, Y. Wang, Y. Huang, X. F. Duan, *Nat. Commun.* **2013**, *4*, 2096.

 © 2020 WILEY-VCH Verlag GmbH & Co. KGaA, Weinheim

[47] Y. F. Hao, M. S. Bharathi, L. Wang, Y. Y. Liu, H. Chen, S. Nie, X. H. Wang, H. Chou, C. Tan, B. Fallahazad, H. Ramanarayan, C. W. Magnuson, E. Tutuc, B. I. Yakobson, K. F. McCarty, Y. W. Zhang, P. Kim, J. Hone, L. Colombo, R. S. Ruoff, *Science* **2013**, *342*, 720.
[48] L. Gan, Z. T. Luo, *ACS Nano* **2013**, *7*, 9480.
[49] W. Guo, F. Jing, J. Xiao, C. Zhou, Y. W. Lin, S. Wang, *Adv. Mater.* **2016**, *28*, 3152.
[50] L. Lin, J. Y. Li, H. Y. Ren, A. L. Koh, N. Kang, H. L. Peng, H. Q. Xu, Z. F. Liu, *ACS Nano* **2016**, *10*, 2922.
[51] H. P. Wang, X. D. Xue, Q. Q. Jiang, Y. L. Wang, D. C. Geng, L. Cai, L. P. Wang, Z. P. Xu, G. Yu, *J. Am. Chem. Soc.* **2019**, *141*, 11004.
[52] J. T. Zhu, H. Xu, G. F. Zou, W. Zhang, R. Q. Chai, J. Choi, J. Wu, H. Y. Liu, G. Z. Shen, H. Y. Fan, *J. Am. Chem. Soc.* **2019**, *141*, 5392.
[53] H. Kim, D. Ovchinnikov, D. Deiana, D. Unuchek, A. Kis, *Nano Lett.* **2017**, *17*, 5056.
[54] W. Chen, J. Zhao, J. Zhang, L. Gu, Z. Z. Yang, X. M. Li, H. Yu, X. T. Zhu, R. Yang, D. X. Shi, X. C. Lin, J. D. Guo, X. D. Bai, G. Y. Zhang, *J. Am. Chem. Soc.* **2015**, *137*, 15632.
[55] J. Y. Chen, W. Tang, B. B. Tian, B. Liu, X. X. Zhao, Y. P. Liu, T. H. Ren, W. Liu, D. C. Geng, H. Y. Jeong, H. S. Shin, W. Zhou, K. P. Loh, *Adv. Sci.* **2016**, *3*, 1500033.
[56] T. R. Wu, X. F. Zhang, Q. H. Yuan, J. C. Xue, G. Y. Lu, Z. H. Liu, H. S. Wang, H. M. Wang, F. Ding, Q. K. Yu, X. M. Xie, M. H. Jiang, *Nat. Mater.* **2016**, *15*, 43.
[57] I. V. Vlassiouk, Y. Stehle, P. R. Pudasaini, R. R. Unocic, P. D. Rack, A. P. Baddorf, I. N. Ivanov, N. V. Lavrik, F. List, N. Gupta, K. V. Bets, B. I. Yakobson, S. N. Smirnov, *Nat. Mater.* **2018**, *17*, 318.
[58] L. L. Patera, F. Bianchini, C. Africh, C. Dri, G. Soldano, M. M. Mariscal, M. Peressi, G. Comelli, *Science* **2018**, *359*, 1243.
[59] J. W. Chung, Z. R. Dai, F. S. Ohuchi, *J. Cryst. Growth* **1998**, *186*, 137.
[60] H. Y. Cun, M. Macha, H. Kim, K. Liu, Y. F. Zhao, T. LaGrange, A. Kis, A. Radenovic, *Nano Res.* **2019**, *12*, 2646.
[61] S. Ishihara, Y. Hibino, N. Sawamoto, H. Machida, H. Wakabayashi, A. Ogura, *MRS Adv.* **2018**, *3*, 379.
[62] S. M. Eichfeld, L. Hossain, Y. C. Lin, A. F. Piasecki, B. Kupp, A. G. Birdwell, R. A. Burke, N. Lu, X. Peng, J. Li, A. Azcatl, S. McDonnell, R. M. Wallace, M. J. Kim, T. S. Mayer, J. M. Redwing, J. A. Robinson, *ACS Nano* **2015**, *9*, 2080.
[63] H. B. Shu, X. S. Chen, X. M. Tao, F. Ding, *ACS Nano* **2012**, *6*, 3243.
[64] T. Ma, W. C. Ren, X. Y. Zhang, Z. B. Liu, Y. Gao, L. C. Yin, X. L. Ma, F. Ding, H. M. Cheng, *Proc. Natl. Acad. Sci. USA* **2013**, *110*, 20386.
[65] X. Z. Xu, Z. H. Zhang, L. Qiu, J. N. Zhuang, L. Zhang, H. Wang, C. N. Liao, H. D. Song, R. X. Qiao, P. Gao, Z. H. Hu, L. Liao, Z. M. Liao, D. P. Yu, E. G. Wang, F. Ding, H. L. Peng, K. H. Liu, *Nat. Nanotechnol.* **2016**, *11*, 930.
[66] C. Liu, X. Z. Xu, L. Qiu, M. H. Wu, R. X. Qiao, L. Wang, J. H. Wang, J. J. Niu, J. Liang, X. Zhou, Z. H. Zhang, M. Peng, P. Gao, W. L. Wang, X. D. Bai, D. Ma, Y. Jiang, X. S. Wu, D. P. Yu, E. G. Wang, J. Xiong, F. Ding, K. H. Liu, *Nat. Chem.* **2019**, *11*, 730.
[67] J. H. Lee, E. K. Lee, W. J. Joo, Y. Jang, B. S. Kim, J. Y. Lim, S. H. Choi, S. J. Ahn, J. R. Ahn, M. H. Park, C. W. Yang, B. L. Choi, S. W. Hwang, D. Whang, *Science* **2014**, *344*, 286.
[68] V. L. Nguyen, B. G. Shin, D. L. Duong, S. T. Kim, D. Perello, Y. J. Lim, Q. H. Yuan, F. Ding, H. Y. Jeong, H. S. Shin, S. M. Lee, S. H. Chae, Q. A. Vu, S. H. Lee, Y. H. Lee, *Adv. Mater.* **2015**, *27*, 1376.
[69] D. Y. Fu, X. X. Zhao, Y. Y. Zhang, L. J. Li, H. Xu, A. R. Jang, S. I. Yoon, P. Song, S. M. Poh, T. H. Ren, Z. Ding, W. Fu, T. J. Shin, H. S. Shin, S. T. Pantelides, W. Zhou, K. P. Loh, *J. Am. Chem. Soc.* **2017**, *139*, 9392.
[70] X. J. Song, J. F. Gao, Y. F. Nie, T. Gao, J. Y. Sun, D. L. Ma, Q. C. Li, Y. B. Chen, C. H. Jin, A. Bachmatiuk, M. H. Ruemmeli, F. Ding, Y. F. Zhang, Z. F. Liu, *Nano Res.* **2015**, *8*, 3164.
[71] J. D. Li, Y. Li, J. Yin, X. B. Ren, X. F. Liu, C. H. Jin, W. L. Guo, *Small* **2016**, *12*, 3645.
[72] M. Q. Zeng, L. X. Wang, J. X. Liu, T. Zhang, H. F. Xue, Y. Xiao, Z. H. Qin, L. Fu, *J. Am. Chem. Soc.* **2016**, *138*, 7812.
[73] X. D. Xue, Q. Xu, H. P. Wang, S. W. Liu, Q. J. Jiang, Z. W. Yu, X. H. Zhou, T. B. Ma, L. P. Wang, G. Yu, *Chem. Mater.* **2019**, *31*, 1231.
[74] J. S. Lee, S. H. Choi, S. J. Yun, Y. I. Kim, S. Boandoh, J. H. Park, B. G. Shin, H. Ko, S. H. Lee, Y. M. Kim, Y. H. Lee, K. K. Kim, S. M. Kim, *Science* **2018**, *362*, 817.
[75] L. Chen, B. L. Liu, M. Y. Ge, Y. Q. Ma, A. N. Abbas, C. W. Zhou, *ACS Nano* **2015**, *9*, 8368.
[76] R. Kappera, D. Voiry, S. E. Yalcin, B. Branch, G. Gupta, A. D. Mohite, M. Chhowalla, *Nat. Mater.* **2014**, *13*, 1128.
[77] A. L. Friedman, A. T. Hanbicki, F. K. Perkins, G. G. Jernigan, J. C. Culbertson, P. M. Campbell, *Sci. Rep.* **2017**, *7*, 3836.
[78] Y. Wang, J. Xiao, S. Yang, Y. Wang, X. Zhang, *Opt. Mater. Express* **2019**, *9*, 1136.
[79] Y. C. Lin, D. O. Dumcencon, Y. S. Huang, K. Suenaga, *Nat. Nanotechnol.* **2014**, *9*, 391.
[80] S. Kretschmer, H. P. Komsa, P. Boggild, A. V. Krasheninnikov, *J. Phys. Chem. Lett.* **2017**, *8*, 3061.
[81] S. Song, D. H. Keum, S. Cho, D. Perello, Y. Kim, Y. H. Lee, *Nano Lett.* **2016**, *16*, 188.
[82] K. A. N. Duerloo, Y. Li, E. J. Reed, *Nat. Commun.* **2014**, *5*, 4214.
[83] D. H. Keum, S. Cho, J. H. Kim, D. H. Choe, H. J. Sung, M. Kan, H. Kang, J. Y. Hwang, S. W. Kim, H. Yang, K. J. Chang, Y. H. Lee, *Nat. Phys.* **2015**, *11*, 482.
[84] G. P. Gao, Y. Jiao, F. X. Ma, Y. L. Jiao, E. Waclawik, A. J. Du, *J. Phys. Chem. C* **2015**, *119*, 13124.
[85] J. Q. Zhu, Z. C. Wang, H. Yu, N. Li, J. Zhang, J. L. Meng, M. Z. Liao, J. Zhao, X. B. Lu, L. J. Du, R. Yang, D. Shi, Y. Jiang, G. Y. Zhang, *J. Am. Chem. Soc.* **2017**, *139*, 10216.
[86] S. J. R. Tan, I. Abdelwahab, Z. J. Ding, X. X. Zhao, T. S. Yang, G. Z. J. Loke, H. Lin, I. Verzhbitskiy, S. M. Poh, H. Xu, C. T. Nai, W. Zhou, G. Eda, B. H. Jia, K. P. Loh, *J. Am. Chem. Soc.* **2017**, *139*, 2504.
[87] Q. M. Huang, X. M. Li, M. H. Sun, L. Zhang, C. Z. Song, L. Zhu, P. Chen, Z. Xu, W. L. Wang, X. D. Bai, *Adv. Mater. Interfaces* **2017**, *4*, 1700171.
[88] T. A. Empante, Y. Zhou, V. Klee, A. E. Nguyen, I. H. Lu, M. D. Valentin, S. A. N. Alvillar, E. Preciado, A. J. Berges, C. S. Merida, M. Gomez, S. Bobek, M. Isarraraz, E. J. Reed, L. Bartels, *ACS Nano* **2017**, *11*, 900.
[89] C. H. Naylor, W. M. Parkin, J. L. Ping, Z. L. Gao, Y. R. Zhou, Y. Kim, F. Streller, R. W. Carpick, A. M. Rappe, M. Drndic, J. M. Kikkawa, A. T. C. Johnson, *Nano Lett.* **2016**, *16*, 4297.
[90] L. Yang, W. F. Zhang, J. Li, S. Cheng, Z. J. Xie, H. X. Chang, *ACS Nano* **2017**, *11*, 1964.
[91] X. L. Xu, S. L. Chen, S. Liu, X. Cheng, W. J. Xu, P. Li, Y. Wan, S. G. Yang, W. T. Gong, K. Yuan, P. Gao, Y. Ye, L. Dai, *J. Am. Chem. Soc.* **2019**, *141*, 2128.
[92] W. Zhao, F. Ding, *Nanoscale* **2017**, *9*, 2301.
[93] H. Xu, D. Han, Y. Bao, F. Cheng, Z. J. Ding, S. J. R. Tan, K. P. Loh, *Nano Lett.* **2018**, *18*, 5085.
[94] Y. F. Yu, G. H. Nam, Q. Y. He, X. J. Wu, K. Zhang, Z. Z. Yang, J. Z. Chen, Q. L. Ma, M. T. Zhao, Z. Q. Liu, F. R. Ran, X. Z. Wang, H. Li, X. Huang, B. Li, Q. H. Xiong, Q. Zhang, Z. Liu, L. Gu, Y. H. Du, W. Huang, H. Zhang, *Nat. Chem.* **2018**, *10*, 638.
[95] L. N. Liu, J. X. Wu, L. Y. Wu, M. Ye, X. Z. Liu, Q. Wang, S. Y. Hou, P. F. Lu, L. F. Sun, J. Y. Zheng, L. Xing, L. Gu, X. W. Jiang, L. M. Xie, L. Y. Jiao, *Nat. Mater.* **2018**, *17*, 1108.
[96] Y. Cao, V. Fatemi, S. Fang, K. Watanabe, T. Taniguchi, E. Kaxiras, P. Jarillo-Herrero, *Nature* **2018**, *556*, 43.
[97] Y. J. Yu, L. G. Ma, P. Cai, R. D. Zhong, C. Ye, J. Shen, G. D. Gu, X. H. Chen, Y. B. Zhang, *Nature* **2019**, *575*, 156.

© 2020 WILEY-VCH Verlag GmbH & Co. KGaA, Weinheim